Transparent Magnetic Photoresists for Bioanalytical Applications

Philip C. Gach[1], **Christopher E. Sims**[1], and **Nancy L. Allbritton**[1,2,*]

[1] Department of Chemistry, University of North Carolina, Chapel Hill, North Carolina 27599

[2] Department of Biomedical Engineering, University of North Carolina, Chapel Hill, North Carolina 27599 and North Carolina State University, Raleigh, North Carolina 27695

Abstract

Microfabricated devices possessing magnetic properties are of great utility in bioanalytical microdevices due to their controlled manipulation with external magnets. Current methods for creating magnetic microdevices yield a low-transparency material preventing light microscopy-based inspection of biological specimens on the structures. Uniformly transparent magnetic photoresists were developed for microdevices that require high transparency as well as consistent magnetism across the structure. Colloidal formation of 10 nm maghemite particles was minimized during addition to the negative photoresists SU-8 and 1002F through organic capping of the nanoparticles and utilization of solvent-based dispersion techniques. Photoresists with maghemite concentrations of 0.01 to 1% had a high transparency due to the even dispersal of maghemite nanoparticles within the polymer as observed with transmission electron microscopy (TEM). These magnetic photoresists were used to fabricate microstructures with aspect ratios up to 4:1 and a resolution of 3 μm. Various cell lines showed excellent adhesion and viability on the magnetic photoresists. An inspection of cells cultured on the magnetic photoresists with TEM showed cellular uptake of magnetic nanoparticles leeched from the photoresists. Cellular contamination by magnetic nanoparticles was eliminated by capping the magnetic photoresist surface with native 1002F photoresist or by removing the top layer of the magnetic photoresist through surface roughening. The utility of these magnetic photoresists was demonstrated by sorting single cells (HeLa, RBL and 3T3 cells) cultured on arrays of releasable magnetic micropallets. 100% of magnetic micropallets with attached cells were collected following release from the array. 85–92% of the collected cells expanded into colonies. The polymeric magnetic materials should find wide use in the fabrication of microstructures for bioanalytical technologies.

Introduction

Materials consisting of both polymers and inorganic particles have been of interest for several decades. These materials possess the ease of processing of polymer substrates along with the integrated benefits of the inorganic phase such as magnetism, conductivity, or luminescence. The use of magnetic particles as a polymer filler has garnered much attention recently due to their utility in biotechnology including cell separations, diagnostics and therapeutic treatments [1–4]. Nanocomposites consisting of a photoresist organic phase and magnetic inorganic phase have found utility in the field of microelectromechanical systems (MEMS) development. These

*Corresponding author. Tel.: +1 919 966 2291; fax: +1 919 962 2388, nlallbri@unc.edu (N.L. Allbritton).

materials would be of great use in developing devices such as micro actuators, sensors, relays and magneto-optical devices based on the Faraday effect. Introduction of magnetic particles into a photosensitive epoxy has been accomplished in recent studies. Damean et al. mixed 100 nm nickel particles at concentrations up to 13% in SU-8, an epoxide-based photoresist, for the purpose of fabricating magnetically actuated microcantilevers [5]. 1–10 μm ferrite particles were introduced into SU-8 to develop microactuators by Hartley and colleagues [6]. Atomic force microscopy probes have been developed by Ingrosso and coworkers by adding maghemite dissolved in toluene to a photoresist [7]. Feldmann and Büttgenbach achieved mixtures of SU-8 with up to 90% ferrites and rare-earth alloys of size 1–10 μm for developing magnetic MEMS [8]. Magnetic rods consisting of 1.8 μm beads have been mixed into SU-8 by Alargova et al. [9]. Dutoit and collaborators blended 10 μm Sm_2Co_{17} particles into SU-8 [10]. SU-8 with magnetite nanoparticles has also been prepared previously [11] [12]. These composite materials possessed either large micrometer-sized structures or aggregated nanoparticles as the magnetic component. These formulations were useful when manufacturing MEMS that did not require uniform magnetism or optical transparency over the entire device. A photoresist with a uniform distribution of magnetic nanoparticles would enable high quality light microscopy of the surfaces as well as uniform forces to be applied across the device during application of a magnetic field.

Nanoparticle self-aggregation in polymers has been minimized in materials such as polydimethylsiloxane (PDMS) [13,14], polymethylmethacrylate (PMMA) [15,16], polystyrene [17], polyimide [18,19], ethyl(hydroxyethyl)cellulose (EHEC) [20] or 3,4-epoxycyclohexylmethyl-3′4′-epoxycyclohexanecarboxylate (CE) but not in an epoxide-based photoresist [21]. The composites were made by capping the nanoparticles with an organic phase or through use of a solvent-based dispersion technique. Peluse et al. integrated magnetic nanoparticles into polystyrene through thermal decomposition of iron mercaptide [17]. Solvent-based dispersion typically involved mixing dilutions of the nanoparticles and polymer separately dissolved in an organic solution, such as chloroform, benzene or toluene, and then evaporating the bulk of the solvent. This method has shown success in dispersing maghemite nanoparticles into PDMS [22] or gold, Diamantane, and single-wall carbon nanotubes (SWNT) into SU-8 [13].

In this study, 10 nm maghemite particles were uniformly distributed into the epoxide-based photoresists SU-8 [23,24] and 1002F [25]. To achieve this, oleic acid-capped maghemite nanoparticles were dissolved in toluene and mixed with the photoresist monomer in toluene. Photoresists with nanoparticle concentrations ranging from 0.01 to 1% maghemite were prepared and nanoparticle distribution aggregation was measured. The UV and visible absorption of the magnetic photoresists was also assessed. Furthermore, microstructures of varying dimensions were formed to determine the achievable resolution and aspect ratios. The ability of cells to attach to and grow on the magnetic photoresists was quantified by culturing 3T3, HeLa and RBL cells on the surfaces. The quality of brightfield and fluorescence microscopy images obtained when illuminating through and collecting light transiting the photoresists was evaluated. The utility of these magnetic structures was demonstrated by using the resist to form micropallet arrays for cell separation and demonstrating collection of released micropallets with cells using a magnetic field [26,27].

Materials and Methods

Magnetic photoresist development

Magnetite nanoparticles were fabricated through the coprecipitation of iron salts in an alkaline medium [28]. The particles were then oxidized to form maghemite nanoparticles by heating in an acidic solution of iron nitrate [29]. The aqueous ferrofluid was then extracted into oleic acid. Excess oleic acid was removed by washing with ethanol. The nanoparticles were then dissolved

in toluene. A 1:5 mixture of 1002F photoresist in toluene was slowly added to a 1:5 dispersion of maghemite nanoparticles in toluene under sonication (Branson 250 sonifier, Danbury, CT). The toluene was then evaporated (Büchi R200 rotovapor, Flawil, Switzerland).

Measurement of photoresist absorption

100 μm-thick films of 1002F photoresist with various concentrations of magnetic nanoparticles were spin-coated onto plasma-cleaned 25 mm-diameter cover glass (Fisher Scientific). Films were then processed identically to that used for pallet fabrication below. Sixteen absorbance measurements were made at various sections of four different films using a SpectraMax M5 (Molecular Devices Corporation, Sunnyvale, CA) with an uncoated cover glass used as a blank. The standard deviation for the transmittance readings was under 5% of the measured value for every data point.

Cell culture

HeLa, 3T3 or RBL cells were cultured in DMEM supplemented with FBS (10%), L-glutamine (584 mg L^{-1}), penicillin (100 units mL^{-1}) and streptomycin (100 μg ml^{-1}) in a 37°C incubator with a 5% CO_2 atmosphere. Before use, cell media was replaced with PBS. Conditioned media was developed by growing subconfluent cultures of HeLa, RBL or 3T3 cells in DMEM supplemented with FBS (10%), L-glutamine (584 mg L^{-1}), penicillin (100 units mL^{-1}) and streptomycin (100 μg ml^{-1}) for 48 hours. The supernatant was centrifuged (3,000×g, 20 min), stored at −20°C and thawed immediately prior to use.

Measurement of cell metabolism

The metabolism of cells growing on photoresists was assessed using the XTT assays as described previously [15]. Adherent HeLa, RBL or 3T3 cells in a logarithmic growth phase were detached from culture plates with 0.05% trypsin and plated on glass, 100 μm-thick 1002F films or 100 μm-thick 1002F films containing 1% magnetic nanoparticles at a density of 5,000 cells/mL (100 μL) and cultured for 24, 48 or 96 hours. XTT assays were then performed on cells as per the manufacturer's instructions (Roche Applied Science, Indianapolis, IN). During a four hour incubation period, active mitochondria from cells will metabolize 2,3-bis(2-methoxy-4-nitro-5-sulfophenly)-5-[(phenylamino) carbonyl]-2H-tetrazolium hydroxide (XTT) to form a water-soluble formazan derivative which is highly absorbent at 480 nm. The contents of four separate chambers were then transferred to a sterile 96 well plate and the absorbance at 480 nm and 650 nm was measured (SpectraMax M5, Molecular Devices Corporation, Sunnyvale, CA).

Transmission electron microscopy (TEM) of cells

100-μm films of SU8 or 1002F photoresists containing nanoparticles were fabricated and coated with fibronectin. HeLa cells at (5,000 cells/mL, 500 μL) were cultured on the surfaces in a 5% CO_2 incubator at 37°C for 48 hours. Cells were washed with 1X PBS buffer 5 times then fixed in Karnovsky's fixative (2.5% glutaraldehyde, 3% paraformaldehyde and 0.1% calcium chloride in 0.1 M sodium cacodylate, pH 7.4) and washed three times with 0.1 M sodium cacodylate buffer. Cells were then placed in 0.05 M osmium tetraoxide in 0.1 M cacodylate buffer for 2 hours followed by 5 changes of distilled water. Cells were then dehydrated by sequential washings in 25%, 50%, 75% and 95% ethanol for 5 minutes each followed by 5 changes of 100% ethanol through infinite dilution for 10 minutes each. Following dehydration, cells were set in a prepared 50:50 mixture of Polybed 812 resin and 100% ethanol overnight followed by 2 changes of 100% Polybed 812 resin for 8 hours and then polymerization at 65°C overnight. Sections of the samples were cut using an ultra microtone, plated on copper grids, and post fixed with uranyl acetate for 15 minutes and lead citrate for 5

minutes followed by three rinses of distilled water. Sections were then observed using a TEM (JEOL 100CX II).

Fabrication of micropallet arrays and PDMS chambers

Magnetic films and pallets were made following protocols reported in prior publications with a few adjustments [25,27]. Briefly, an oven at 95°C was used for all pre-baking and post-baking steps in place of a hotplate. Magnetic photoresists containing 1% magnetic nanoparticles require approximately 10x higher UV illumination intensities during fabrication relative to that of native 1002F pallets. During long exposure times an aluminum block was placed beneath the glass slide to dissipate heat.

Following pallet fabrication, a PDMS ring was attached to the surface of the pallet array with PDMS. Virtual air walls were then developed through chemical vapor deposition of a hydrophobic perfluoroalkylsilane layer on the silicone oxide surface as described previously [27]. Prior to loading with cells, pallet arrays and films were sterilized through rinsing with 95% ethanol and dried in a tissue culture hood. Excess ethanol was removed with five PBS rinses. Top surfaces of the pallets on the array were then coated with 1 mL of 25 µg/mL fibronectin in PBS for four hours at room temperature. Following surface coating the array was rinsed five times with 1X PBS. 1X PBS was replaced with cell culture media and suspensions of HeLa, 3T3 or RBL cells were added to the array to yield <1 cell per pallet (1mL of 30,000 cells for $50\times50\times50$ μm^3 pallets and 1mL of 15,000 cells for $100\times100\times50$ μm^3 pallets). Cells were allowed to settle and adhere onto single pallets. Six hours later, cells were imaged and pallets released and collected in 1X PBS. After cell/pallet collection, the PBS was replaced with conditioned medium.

Released pallets were collected onto a substrate attached to the pallet array by a PDMS ring and an O-ring. For these studies the collection substrate was composed of a multiwell PDMS plate as described previously [26]. A silicon O-ring (24 mm outer diameter, McMaster-Carr, Los Angeles, CA) was attached to the collection substrate using PDMS to provide a fluid chamber for culture media. Prior to use for cell collection, the collection chamber was autoclaved, rinsed with ethanol and washed with PBS ten times. Following sterilization, the PDMS multiwell plate was treated with 25 µg/mL fibronectin in 1X PBS for six hours at room temperature.

Supplemental materials and methods

Details are supplied in the Supplemental materials for the following: reagents, scanning electron microscopy (SEM), laser-based release of pallets and magnetic field characterization.

Results and Discussion

Development of magnetic photoresists

Superparamagnetic maghemite nanoparticles were used for manufacturing magnetic microstructures because of their small size, controllable magnetism and biological compatibility [30]. Ten-nm magnetite nanoparticles were fabricated through the Massate method and then oxidized to maghemite to provide stability in an oxygen environment [28, 29]. Oleic acid was added to the nanoparticles which then formed a stable ferrofluid in toluene at concentrations below 5% (Fig. S1) [31]. When this ferrofluid was mixed into SU-8 or 1002F negative photoresist, large colloids formed due to the nanoparticle's preference for self-adhesion (Fig. S2). To prevent this aggregation, both the photoresist and ferrofluid were diluted into toluene prior to mixing. A mixture of SU8 or 1002F photoresist in toluene was slowly added to the maghemite nanoparticles under sonication. The mixture was then heated to evaporate the toluene. Films of varying thicknesses were then fabricated from the magnetic

photoresists. To fully cure, photoresists with maghemite nanoparticles required 2 to 10 times higher UV illumination intensities than that of the native photoresists. The uniformity of the nanoparticle distribution in the photoresist was assessed by transmission electron microscopy (TEM) of films fabricated from photoresists with 1% maghemite particles. The TEM images confirmed the lack of colloid formation during the fabrication process with retention of the small nanoparticle size (10±5 nm, n=77) (Fig. 1A, B). The maghemite nanoparticles were stably suspended in 1002F or SU8 at concentrations up to 1% with minimal aggregation for over six months.

Absorbance of magnetic photoresists

Many biomedical applications require a transparent photoresist for visualization of structures such as cells or other features above or below the photoresist or for measurement of light-based signals such as absorbance or fluorescence. To determine whether the photoresist with maghemite particles was transparent, the transmittance of 1002F films possessing varying concentrations of maghemite particles was measured (Fig. 1C). The transmittance in the shorter wavelengths decreased as the concentration of magnetic nanoparticles was increased. The decreased UV transparency was the most likely reason for the increased illumination intensities required to fully cure the polymeric photoresist. An 80% light transmittance was observed for resists with 0.1–1% particles at 458–572 nm, respectively. Thus transparency was excellent at the longer visible wavelengths frequently used for biomedical assays and imaging. SU8 films with nanoparticles yielded similar transmittance curves to that of 1002F films with identical nanoparticle concentrations (data not shown).

Cell growth on magnetic photoresists

Photoresists are commonly used as substrates for cell culture on devices targeted towards biomedical research [32–34]. The metabolism of cell cultures grown on photoresists with and without maghemite nanoparticles and on a standard tissue culture surface was compared for three cell lines (HeLa, RBL and 3T3) (Figure 2). Identical numbers of cells were plated on each of the surfaces for these measurements. Cell cultures grown on glass slides possessed a slightly greater metabolic rate than those grown on the photoresists. This may be due to either a faster growth rate or greater mitochondrial activity of the cells on glass. Cell cultures grown on native 1002F or magnetic 1002F possessed similar metabolic rates (two sided t-test on 96 hr values, [HeLa] $t(6)=0.831$, $p=0.4$, [RBL] $t(6)=0.425$, $p=0.7$, [3T3] $t(6)=1.866$, $p=0.1$). These results demonstrated that the maghemite nanoparticles possessed minimal effects on the short term growth of cells. The small decrease in the metabolic activity of cell cultures grown on photoresists relative to that on glass may be due to the greater hydrophobicity of 1002F and consequently reduced cell adhesion to 1002F compared to that on glass [25].

There is much controversy as to the influence of cellular nanoparticle uptake on the health and well being of cells and tissues [35–38]. Thus presence of maghemite nanoparticles within cells grown on the nanoparticle-containing surfaces would be an undesired consequence. To determine whether particles accumulated in cells in contact with the surfaces, HeLa cells were cultured on 100-μm thick films of SU8 and 1002F with and without 1% dispersed maghemite particles. Following fixation and staining, sections of the cells were imaged by TEM. HeLa cells cultured on the photoresist with nanoparticles (but not those on standard 1002F) possessed large aggregates of the magnetic nanoparticles within the cytoplasm (Figure 3A). To understand how cells might come into contact with the nanoparticles, vertical sections of photoresist with 1% maghemite nanoparticles were examined by TEM. Nanoparticles were observed to be at high density near the surface of the photoresist (Figure 3B). Evaporation of solvent during the baking process may have transported the particles to the surface of the photoresist. It was likely that these surface nanoparticles were those taken up by the cells. To reduce the high density of nanoparticles on the photoresist surface, two approaches were tested.

The first strategy was to apply a 2-μm layer of 1002F without nanoparticles over the magnetic photoresist to provide a barrier between the cells and the magnetic photoresist surface. HeLa cells cultured on this barrier surface above the magnetic photoresist did not possess identifiable nanoparticles within their cytoplasm as demonstrated by TEM (Figure 3C). Alternatively, the surface of the magnetic photoresist was roughened for 30 minutes, as described previously, to remove the photoresist near the surface of the films and thus the high density region of nanoparticles [39]. Vertical slices of the roughened magnetic photoresists (1% maghemite) were obtained and imaged with TEM. The high density layer of nanoparticles was fully removed by the roughening process (Figure 3D). When HeLa cells cultured on these films were examined by TEM, the cells did not possess identifiable cytoplasmic nanoparticles (data not shown). Thus both strategies, a barrier coating or surface nanoparticle removal, eliminated nanoparticle uptake by the cells.

Imaging cells on magnetic photoresists

A uniform dispersion of magnetic nanoparticles in polymers is required for high quality cell imaging by optical microscopy. To compare the image quality of cells on photoresists containing aggregated and uniformly distributed nanoparticles, RBL cells were cultured on: glass, 5 and 50 μm thick films of 1002F or SU8, 5 and 50 μm thick films of 1002F or SU8 containing 1% dispersed maghemite nanoparticles and 5 and 50 μm thick films of 1002F or SU8 containing 1% aggregated maghemite nanoparticles. RBL cells, which possess Fcε receptors, were incubated with AlexaFluor 647-labeled IgE. Cells cultured on the various substrates were then imaged by brightfield and fluorescence microscopy. Cells cultured on glass, 1002F, SU8, or 1002F/SU-8 (5 and 50 μm films) with uniformly distributed maghemite nanoparticles were clearly visualized by brightfield microscopy (Figure 4A and B). When cells were cultured on 1002F or SU8 photoresists (5-μm films) containing aggregated maghemite nanoparticles and examined by brightfield microscopy, portions of the cells were obscured by the particle aggregates and thus not visualized (Figure 4C). When cells on these surfaces were imaged by fluorescence microscopy, a halo of scattered light surrounded the cells and much of the cell's interior appeared jagged and irregular (Figure S3). Cells cultured on thicker films of photoresists (50-μm films) containing aggregated nanoparticles were not identifiable (Figure S3). Uniformity in the distribution of magnetic nanoparticles throughout the photoresists is a critical to obtain quality images of cells with either brightfield or fluorescence microscopy.

Formation of microstructures with the magnetic photoresist

For widespread utility, a photoresist must be capable of forming microstructures with good aspect ratios and micron-sized resolution. To evaluate whether microstructures could be formed, a test pattern possessing structures ranging in size from 2 to 20 μm was used to form microstructures from photoresists with 1% dispersed maghemite particles. Square and circular microstructures with dimensions of 3 to 20 μm possessed sharp side walls when formed from either 1002F or SU-8 photoresist with 1% maghemite nanoparticles (Figure 5A–C). Microstructures with thicknesses between 5 and 100 μm were also successfully fabricated. An aspect ratio of 4:1 was achieved with both of the magnetic photoresists (Figure 5B and C). This is comparable to the aspect ratio of 4:1 achieved with native 1002F photoresist and 5:1 with SU-8 under similar fabrication conditions [25]. Successful formation of microstructures with various dimensions demonstrates the feasibility of further micro device development with the magnetic photoresists.

Magnetic manipulation of microstructures

The utility of magnetic microstructures lies in their ability to be manipulated by an external magnetic field. Magnetic cantilevers, micro actuators, microstir bars and micropallets are a few examples of structures in which a high magnetic response would be desirable in a

microstructure [5,40,41]. The ability to manipulate micro structures formed from a magnetic photoresist was analyzed by fabricating micropallets from 1002F with 1% maghemite particles and using an external magnetic field to collect the structures released from a surface. To determine whether pallet collection using a magnetic force might be possible, the gravitational force (F_g, Equation 1) and magnetic force (F_m, Equation 2) on a micropallet was estimated.

$$F_g = mg \tag{1}$$

$$F_m = \frac{V \cdot \Delta \chi}{\mu_o} (B \cdot \nabla) B \tag{2}$$

m is the mass of a pallet, g is the acceleration due to gravity, V is the volume of magnetic particles (m^3), $\Delta\chi$ is the difference in the magnetic susceptibilities between the of nanoparticle and the surrounding medium, B is the magnetic field strength and μ_o is the permeability of vacuum. The effects of viscous drag were neglected in these equations. As an example, $100 \times 100 \times 100$ μm^3 pallet with 1% magnetic nanoparticles experiences a gravitational force of 12 nN. Under a typical magnetic field strength of 50 mT (generated by a small permanent magnet), the magnetic force on the pallet would be 40 nN. This suggests that the microstructures can easily be collected against the force of gravity.

To demonstrate the ability to collect microstructures, the collection of individual micropallets from an array was used. Micropallet technology utilizes an array of 10^3–10^6 releasable platforms, each large enough to fit a single cell or a colony of cells. After selective identification, the pallet of interest can be detached from the substrate with a laser pulse and collected. The efficiency of micropallet collection following release from an array was measured as a function of pallet size, magnetic nanoparticle content and magnetic field strength. The magnetic field strength was altered by varying the distance of the micropallet array from a permanent magnet. Arrays composed of either $50 \times 50 \times 50$ μm^3 or $100 \times 100 \times 100$ μm^3 pallets fabricated from 1002F containing 0 to 1% magnetic nanoparticles were utilized. A PDMS ring ranging in thickness from 0.5 mm to 21 mm was placed around the array and then filled with PBS. A glass coverslip (0.017 mm thick) with attached magnet was placed in contact with the PBS. The number of pallets collected on the glass coverslip surface adjacent to the magnet following laser-based pallet release from the array was measured. Pallets with 1% maghemite were readily collected when the magnetic strength field in the array plane was 449 to 43 mT corresponding to a coverslip distance of 1 to 15 mm above the array (Table 1, Figure 5D–F). In contrast pallets of photoresist without nanoparticles could not be collected on the coverslip when the coverslip was placed 1 to 15 mm above the array. In this instance the released pallet settled back onto the array surface. Notably micropallets with as little as 0.1% maghemite could be collected with 100% efficiency for magnetic strength fields in the array plane of 449 to 204 mT corresponding to coverslip distances of 1 to 5 mm. Pallets with 0.01% maghemite particles could also be collected although at reduced efficiency. Not surprisingly collection efficiency was independent of pallet size since the pallet and nanoparticle mass scaled proportionally as pallet size increased.

In addition to collecting magnetic devices vertically, magnetic manipulation may be an efficient method for collection of microstructures in a horizontal direction. The feasibility of a horizontal collection method was tested by placing a Nd magnet axially against an array of $50 \times 50 \times 50$ μm^3 square pallets developed from 1002F and containing a concentration of 1% maghemite. Pallets were released (triplicate data sets were n=10) at various distances from the

magnet (2 to 20 mm) and the percentage of released pallets collected on a PDMS surface adjacent to the magnet was assessed. A 100% collection efficiency was observed for magnetic pallets released at distances of 2 to 12 mm from magnet, representing a magnetic field strength of 390 to 60 mT. A Nd magnet-separation of 14 mm (47 mT) from the magnet produced a pallet collection efficiency of 77 ± 12 % and pallets released at a distance of 16 mm (38 mT) from the external magnet had a probability of collection of 3 ± 12 %. No magnetic pallets greater than 18 mm (30 mT) from the external magnet were collected. These results demonstrate that the magnetic microstructures can be collected with very high efficiency using magnetic forces parallel or perpendicular to the force of gravity. Prior collection methods for the micropallets yielded maximal collection efficiencies ranging between 10 to 63% of the released pallets [26].

Separating cells using magnetic pallet arrays

Previously, arrays of micropallets have been demonstrated to be ideal platforms for culture and then separation of cells [26]. To determine whether the magnetic micropallet arrays might also be used to separate cells, HeLa, RBL or 3T3 cells were cultured on these arrays at a density of <1 cell/pallet (Figure 6D). The arrays were fabricated from pallets (50 μm side, 30 μm height) composed of 1002F with 0.1 or 1% maghemite nanoparticles. Pallets were collected using the vertical format with a Nd magnet placed over a multiwell collection plate under conditions that yield a 100% pallet collection efficiency. Following collection, the cells were placed in an incubator for 100 hours and the number of cells that formed a colony was counted. The percentage of collected single HeLa, RBL or 3T3 cells that survived collection and expanded into a colony was $90 \pm 7\%$, $87 \pm 10\%$ and $87 \pm 9\%$, respectively for magnetic pallets with 0.1% magnetic nanoparticles. Similarly, colony formation of released HeLa, RBL or 3T3 cells was $88 \pm 6\%$, $92 \pm 6\%$ and $85 \pm 4\%$, respectively for magnetic pallets containing 1% maghemite. The survival of cells collected with magnetic pallets was consistent with the values recorded for cells successfully collected with non-magnetic pallets [26]. However in these prior reports a maximum of 63% of released non-magnetic micropallets could be collected. The combined high collection efficiency and high survival rate of cells on magnetic pallets makes this magnetic arrays attractive for applications in which all identified cells must be collected i.e. isolation of rare cells from a population.

Conclusions

Transparent magnetic photoresists have been developed, characterized and their utility a bioanalytical application demonstrated. Ten-nm maghemite nanoparticles were successfully distributed into 1002F and SU8 photoresists with minimal aggregation at concentrations up to 1%. These photoresists retained their transparency at long wavelengths. The magnetic photoresists have been used to successfully create microstructures with sizes ranging from 3 to 100 μm. Uptake of nanoparticles by cells cultured on the photoresists was eliminated by capping with a native photoresist or by removal of the photoresist top layer which possessed concentrated nanoparticles. The metabolic activity of cells cultured on the magnetic photoresist was similar to that of cells grown on native photoresist. Manipulation of the magnetic microstructures by an external field was demonstrated by collection of micropallets with and without cells. These polymeric magnetic materials should find wide use in the fabrication of structures for BioMEMS applications such as magnetic cell arrays, micro actuators, magnetic cantilevers, magnetic AFM probes, stir bars, sensors, relays and magneto-optical devices.

Supplementary Material

Refer to Web version on PubMed Central for supplementary material.

Acknowledgments

References

1. Duguet E, Vasseur S, Mornet S, Devoisselle JM. Magnetic nanoparticles and their applications in medicine. Nanomedicine (London, England) 2006;1(2):157–168.

2. Kumano S, Murakami T, Kim T, Hori M, Okada A, Sugiura T, et al. Using superparamagnetic iron oxide-enhanced MRI to differentiate metastatic hepatic tumors and nonsolid benign lesions. AJR Am J Roentgenol 2003;181:1335–1339. [PubMed: 14573430]

3. Amirfazli A. Magnetic nanoparticles hit the target. Nature Nanotechnol 2007;2:467–468. [PubMed: 18654342]

4. Prasad NK, Rathinasamy K, Panda D, Bahadur D. Mechanism of cell death induced by magnetic hyperthermia with nanoparticles of γ–$Mn_\chi Fe_{2-\chi}O_3$ synthesized by a single step process. J Mater Chem 2007;17:5042–5051.

5. Damean N, Parviz BA, Lee JN, Odom T, Whitesides GM. Composite ferromagnetic photoresist for the fabrication of microelectromechanical systems. J Micromech Microeng 2005;15:29–34.

6. Hartley AC, Miles RE, Corda J, Dimitrakopoulos N. Large throw magnetic microactuator. Mechatronics 2008;18:459–465.

7. Ingrosso C, Martin C, Llobera A, Perez Murano F, Innocenti C, Sangregorio C, et al. Magnetic nanocrystals modified epoxy photoresist for microfabrication of AFM probes. Procedia Chem 2009;1:580–584.

8. Feldmann M, Büttgenbach S. Novel microrobots and micromotors using Lorentz force driven linear microactuators based on polymer magnets. IEEE Trans Magn 2007;43:3891–3895.

9. Alargova RG, Paunov VN, Velev OD. Formation of polymer microrods in shear flow by emulsification solvent attraction mechanism. Langmiur 2006;22:765–774.

10. Dutoit BM, Besse PA, Blanchard H, Guérin L, Popovic RS. High performance micromachined Sm_2Co_{17} poymer bonded magnets. Sens Actuators A Phys 1999;77:178–182.

11. Wiche G, Goettert J, Song Y, Hormes J, Kumar CSSR. Functional micro devices using 'nanoparticle-photoresist' composites. IJCES 2003;4:525–528.

12. Suter M, Graf S, Ergeneman O, Schmid S, Camenzid A, Nelson BJ, Hierold C. Superparamagnetic photosensitive polymer nanocomposite for microactuators. Transducers IEEE 2009:869–872.

13. Chiamori HC, Brown EV, Adhiprakasha ET, Straalsund JB, Melosh NA, Pruitt BL. Suspension of nanoparticles in SU-8 and characterization of nanocomposite polymers. ENS'05 2005:14–16.

14. Yamanishi Y, Sakuma S, Arai F. Production and application of high-accuracy polymer-based magnetically driven microtool. J Robot Mechatron 2008;20:274–279.

15. Li S, Qin J, Fornara A, Toprak M, Muhammed M, Kim DK. Synthesis and magnetic properties of bulk transparent PMMA/Fe-oxide nanocomposites. Nanotech 2009;20:185607.

16. Gass J, Poddar P, Almand J, Srinath S, Srikanth H. Superparamagnetic polymer nanocomposites with uniform Fe_3O_4 nanoparticle dispersions. Adv Funct Mat 2005;16:71–75.

17. Peluso A, Pagliarulo V, Carotenuto G, Pepe GP, Davino D, Visone C, et al. Synthesis and characterization of polymer embedded iron oxide nanocomposites. Microw Opt Technol Let 2009;51:2774–2777.

18. Lagorce LK, Allen MG. Magnetic and mechanical properties of micromachined strontium ferrite/polyimide composites. J Microelectromech Syst 1997;6:307–312.

19. Rojanapornpun O, Kwok CY. Fabrication of integrated micromachined polymer magnet. Proc Of SPIE 2004;4592:347–354.

20. Hayashi K, Fujikawa R, Sakamoto W, Inoue M, Yogo T. Synthesis of highly transparent lithium ferrite nanoparticle/polymer hybrid self-standing films exhibiting faraday rotation in the visible region. J Phys Chem C 2008;112:14255–14251.

21. Sangermano M, Priola A, Kortaberria G, Jimeno A, Garcia I, Mondragon I, Rizza G. Photopolymerization of epoxy coatings containing iron-oxide nanoparticles. Macromol Mater Eng 2007;292:956–961.

22. Evans BA, Shields AR, Lloyd Carrol R, Washburn S, Falvo MR, Superfine R. Magnetically actuated nanorod arrays as biomimetic cilia. Nano Lett 2007;7:1428–1438. [PubMed: 17419660]

23. Shaw JM, Gelorme JD, LaBianca NC, Conley WE, Holmes SJ. Negative photoresist for optical lithography. IBM J Res Dev 1997;41:81–94.

24. Gelmorme, JD.; Cox, RJ.; Gutierrez, SA. Photoresist Composition and Printed Circuit Boards and Packages Made Therewith. (IBM). US Patent. 4882245. 1989.

25. Pai J-H, Wang Y, Salazar GTA, Sims CE, Bachman M, Li GP, Allbritton NL. Photoresist with low fluorescence for bioanalytical applications. Anal Chem 2007;79:8774–8780. [PubMed: 17949059]

26. Wang Y, Young G, Bachman M, Sims CE, Li GP, Allbritton NL. Collection and expansion of single cells and colonies released from a micropallet array. Anal Chem 2007;79:2359–2366. [PubMed: 17288466]

27. Wang Y, Sims CE, Marc P, Bachman M, Li GP, Allbritton NL. Micropatterning of living cells on a heterogeneously wetted surface. Langmuir 2006;22:8257–8262. [PubMed: 16952271]

28. Massart R. Preparation of aqueous magnetic liquids in alkaline and acidic media. IEEE Trans Magn 1981;17:1247–1248.

29. Bee A, Massart R, Neveu S. Synthesis of very fine maghemite particles. J Magn Magn Mater 1995;149:6–9.

30. Pamme N. Magnetism and microfluidics. Lab Chip 2006;6:24–38. [PubMed: 16372066]

31. van Ewijk GA, Vroege GJ, Philipse AP. Convenient preparation methods for magnetic colloids. J Magn Magn Mater 1999;201:31–33.

32. Heuschkel MO, Guerin L, Buisson B, Bertrand D, Renaud P. Buried microchannels in photopolymer for delivering of solutions to neurons in a network. Sens Actuators B Chem 1998;48:356–361.

33. Kotzar G, Freas M, Abel P, Fleishman A, Roy S, Zorman C, et al. Evaluation of MEMS materials of construction for implantable medical devices. Biomaterials 2002;23:2737–2750. [PubMed: 12059024]

34. Voskerician G, Shive MS, Shawgo RS, Recum HV, Anderson JM, Cima MJ, Langer R. Biocompatibility and biofouling of MEMS drug delivery devices. Biomaterials 2003;24:1959–1967. [PubMed: 12615486]

35. Häfeli UO, Riffle JS, Harris-Shekhawat L, Carmichael-Baranauskas A, Mark F, Dailey JP, Bardenstein D. Cell uptake and in vitro toxicity of magnetic nanoparticles sutable for drug delivery. Mol Pharm 2009;6:1417–1428. [PubMed: 19445482]

36. Gupta AK, Naregalkar RR, Vaidya VD, Gupta M. Recent advances on surface engineering of magnetic iron oxide nanoparticles and their biomedical applications. Nanomedicine (London, England) 2007;2(1):23–39.

37. Jain TK, Reddy MK, Morales MA, Leslie-Pelecky DL, Labhasetwar V. Biodistribution, clearance, and biocompatibility of iron oxide magnetic nanoparticles in rats. Mol Pharm 2008;5:316–327. [PubMed: 18217714]

38. Gupta A, Gupta M. Cytotoxicity suppression and cellular uptake enhancement of surface modified magnetic nanoparticles. Biomaterials 2005;26:3995–4021. [PubMed: 15626447]

39. Shadpour H, Sims CE, Thresher RJ, Allbritton NL. Sorting and expansion of murine embryonic stem cell colonies using micropallet arrays. Cytometry 2009;75A:121–129. [PubMed: 19012319]

40. Lu LH, Ryu KS, Liu C. A magnetic microstirrer and array for microfluidic mixing. J Microelectromech Syst 2002;11(3):462–469.

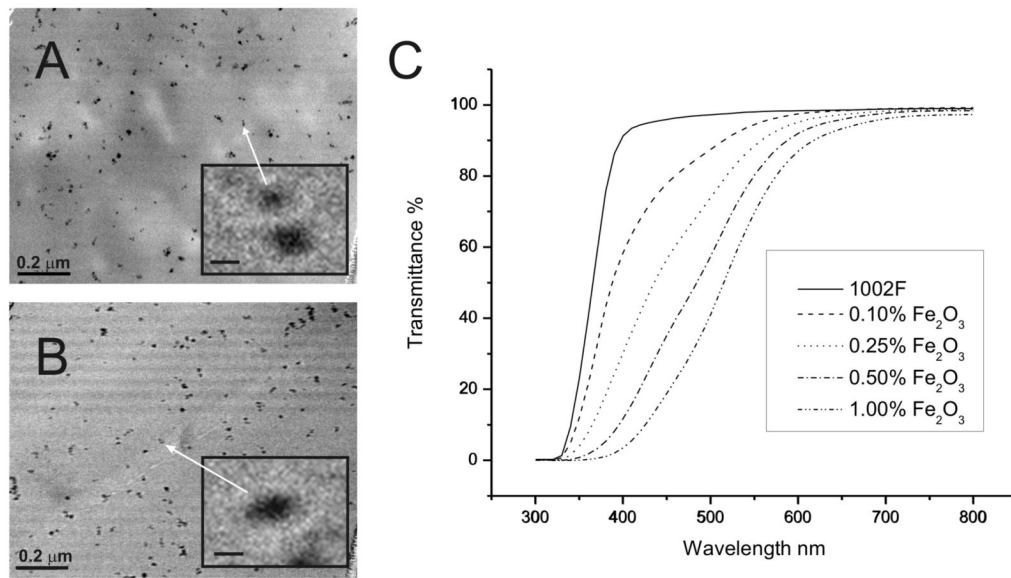41. Cugat O, Delamare J, Reyne G. Magnetic micro-actuators and systems (MAGMAS). IEEE Trans Magn 2003;39(5):3607–3612.

Figure 1.
Photoresists with dispersed maghemite nanoparticles. TEM images of 1% maghemite nanoparticles in 1002F (A) or SU-8 (B) photoresists (scale bar is 200 nm). Insert shows an expanded view of a single nanoparticle (scale bar is 10 nm). Transmittance of 100 μm thick films of 1002F with various concentrations of magnetic nanoparticles (C).
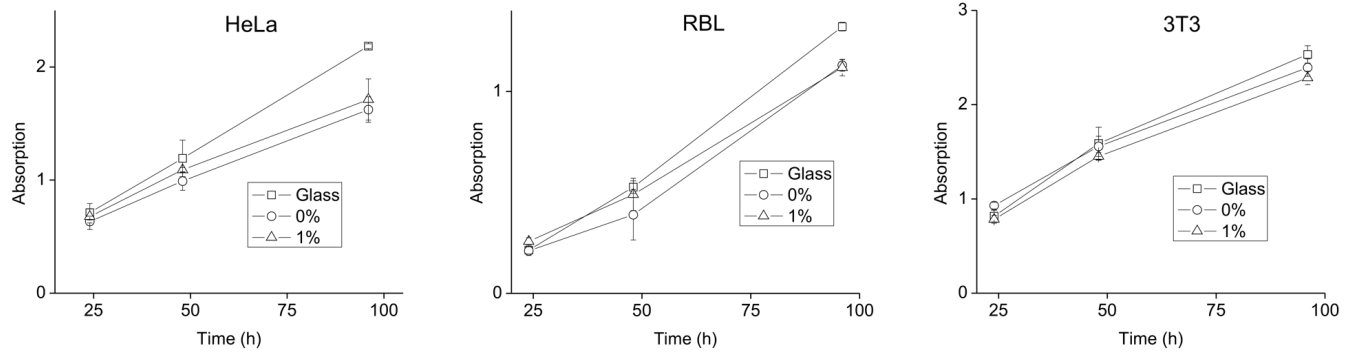
Figure 2.
Measurement of metabolism by colorimetric assay of cells grown on photoresist. HeLa, RBL or 3T3 cells were cultured on glass (squares), 1002F photoresist (circles), or 1002F photoresist with 1% maghemite nanoparticles (triangles) for varying times. Shown on the "y" axis is the absorbance of the orange formazon product produced by metabolically active cells. Error bars represent the standard deviation of four measurements.
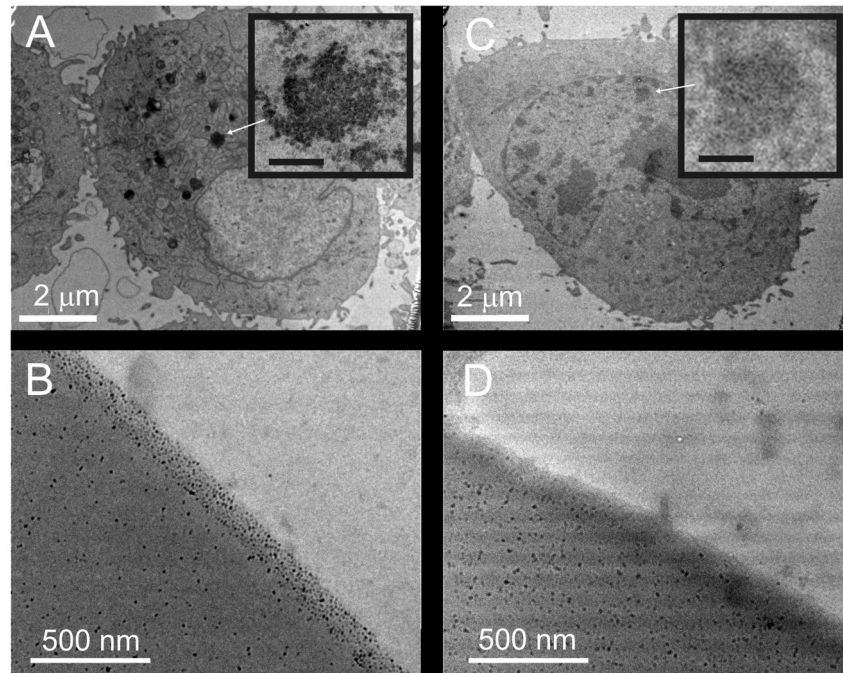
Figure 3.
Uptake of maghemite nanoparticles by cells. TEM images of HeLa cells cultured on 1% magnetic 1002F without (A) and with (C) a 2 μm-thick protective film of native 1002F over the magnetic photoresist. Arrows show clusters of nanoparticles within the cells. Inserts show enlarged images of the magnetic nanoparticles (A) and cellular organelles without nanoparticles (C) (scale bars are 150 nm). TEM images of 1002F photoresist containing 1% maghemite nanoparticles before (B) and after surface roughening (D).
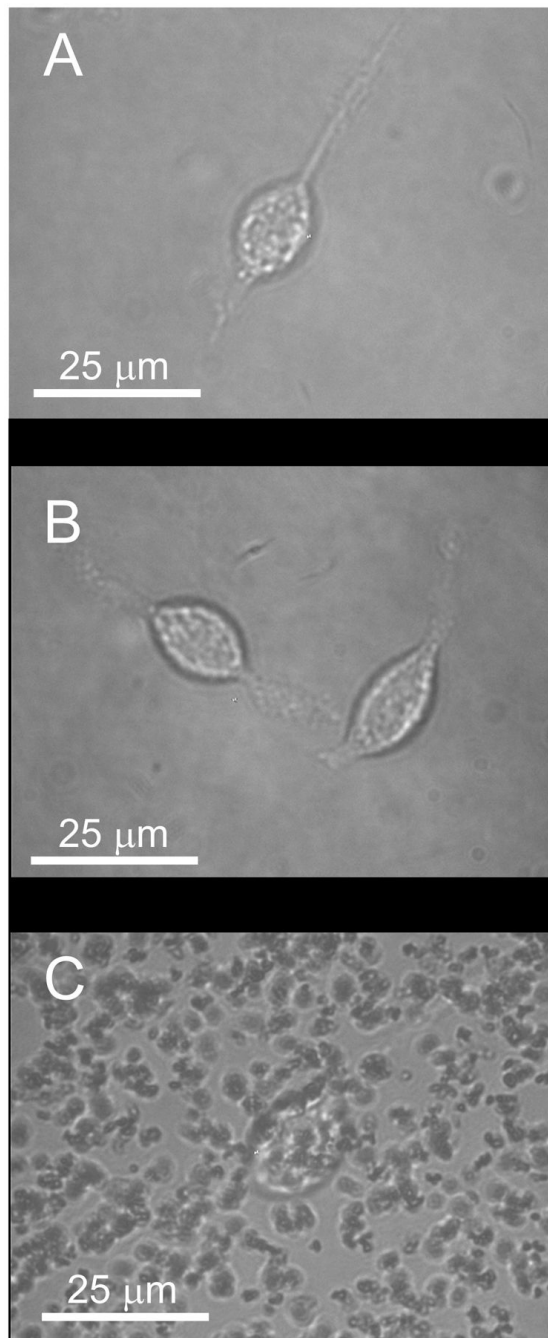
Figure 4.
Brightfield images of photoresists with attached RBL cells. The 5-μm thick films were comprised of 1002F (A), 1002F with 1% maghemite particles uniformly dispersed (B), and 1002F with 1% maghemite particles aggregated (C).
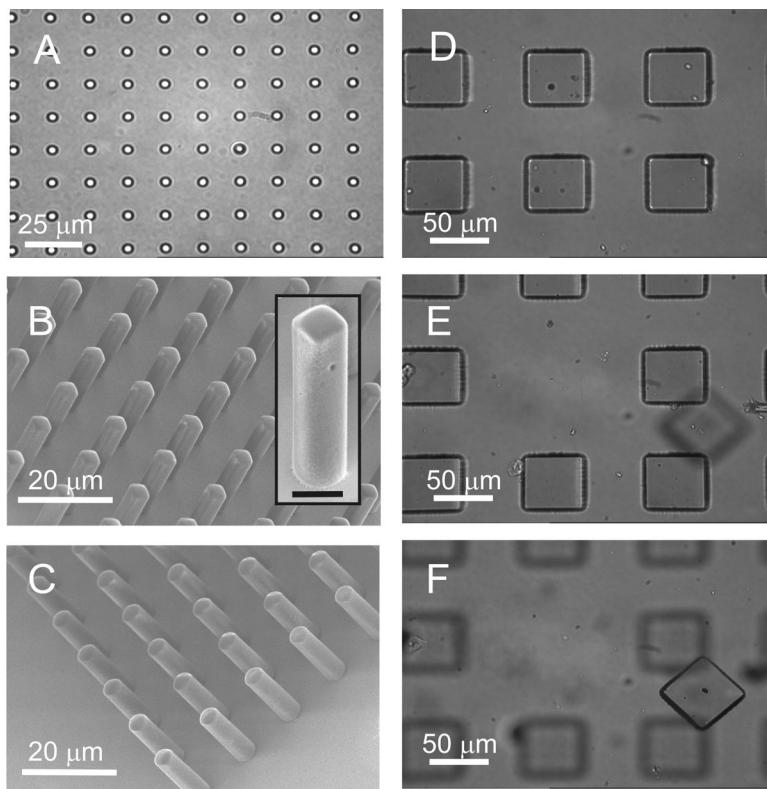
Figure 5.
Microstructures from magnetic photoresists. Brightfield image of 3 μm circular structures composed of SU8 with 1% maghemite nanoparticles (A). SEM images of rectangular structures formed from 1002F photoresist containing 1% maghemite nanoparticles (B) and cylindrical structures formed from SU-8 photoresist containing 1% maghemite nanoparticles (C). The microstructures in B and C were fabricated from masks with 3 μm-sized openings and film heights of 12 μm. Insert shows an expanded view of a single rectangular structure (scale bar is 5 μm). Brightfield image of an array prior to laser-based release of a pallet (D). The pallets were $100\times100\times30$ μm^3 in size and composed of 1002F with 1% maghemite nanoparticles. At the array surface the magnetic field was 502 mT. (E) Image of the same array after pallet release. The objective focal plane is located at in the plane of the array. (F) Image of the released pallet. The objective focal plane is located on the glass slide 0.5 mm above the array.

Table 1

Vertical Collection of Magnetic Micropallets

% Fe_2O_3	Pallet/Magnet Separation (mm)	B Field at Pallet Array (mT)	Collection Probability (%) 50×50×50 μm³	Collection Probability (%) 100×100×100 μm³
0	0.5	502 ± 5	10 ± 5	0 ± 0
0.01	0.5	502 ± 5	93 ± 8	55 ± 15
	1	449 ± 4	3 ± 3	0 ± 0
0.10	1	449 ± 4	100 ± 0	100 ± 0
	5	204 ± 11	100 ± 0	100 ± 0
	9	94 ± 4	23 ± 8	17 ± 8
1.00	1	449 ± 4	100 ± 0	100 ± 0
	5	204 ± 11	100 ± 0	100 ± 0
	9	94 ± 4	100 ± 0	100 ± 0
	12	60 ± 2	100 ± 0	100 ± 0
	15	43 ± 3	100 ± 0	100 ± 0
	18	30 ± 2	65 ± 13	73 ± 25
	21	21 ± 2	3 ± 3	8 ± 6

Triplicate experiments (n=20 pallets per experiment).